

Master–Slave double–scroll circuit incomplete synchronization

I. M. Kyprianidis, Ch. K. Volos, S. G. Stavriniades*, I. N. Stouboulos and A. N. Anagnostopoulos

Physics Department, Aristotle University of Thessaloniki, GR-54124, Greece.

Received 29 January 2010; Accepted 17 March 2010

Abstract

The experimental study of the route from synchronization to desynchronization of a master-slave configuration of double-scroll circuits, is presented. The parameter controlling the system synchronization was the coupling resistance between the master-slave circuits. In the region between synchronization-desynchronization, it was shown that an intermediate regime of incomplete synchronization emerged. The study of the related dynamics proved that this incomplete synchronization was of the on-off intermittency kind.

Keywords: Synchronization, unidirectional coupled nonlinear circuits, double-scroll circuit, incomplete synchronization, intermittency.

1. Introduction

Over the last decades the study of chaotic oscillators has emerged as an object of great interest in many scientific fields [1-2]. An important research activity has been devoted to the dynamics of coupled chaotic oscillators. The discovery, that chaotic systems can be synchronized [3], can be considered as a key event for the research and application of chaotic systems [4]. It has inspired a number of chaos-based master-slave systems, in particular for broadband communication applications [5-8] and cryptography [9-14].

It has been known, that many nonlinear functions can generate chaos. Typical examples are piecewise-linear functions (e.g. Chua's circuit) [15], the smooth cubic function (e.g. the Duffing oscillator) [16], the smooth quadratic function (e.g. the Lorenz system) and the piecewise-quadratic function [17-18]. Among them Chua's circuit is a paradigm for chaos, being a simple nonlinear electrical circuit that exhibits double scroll chaotic attractors. An alternative way for generating double scroll like behavior was proposed by means of a simple circuit implementation [19-20]. Recently, a double scroll electronic circuit, based on a saturated function, was presented [21].

The synchronization phenomenon between nonlinear chaotic circuits has been studied intensively [22-24]. However, the route from synchronization to desynchronization and the corresponding statistics, have not been experimentally studied, but only in a few cases [25-29]. In this paper, the case of on-off intermittent synchronization (also termed incomplete synchronization) between two identical double scroll circuits was studied. The two circuits were resistively coupled in a unidirectional way, forming a master-slave configuration.

2. The electronic circuits

In Fig.1 two identical nonlinear double scroll circuits are connected, via an op-amp buffer (numbered 7) and a linear resistor R_C , implementing a unidirectional coupling. Apparently, the realized circuit system forms a master–slave configuration. The state equations, describing the normalized equation system, are:

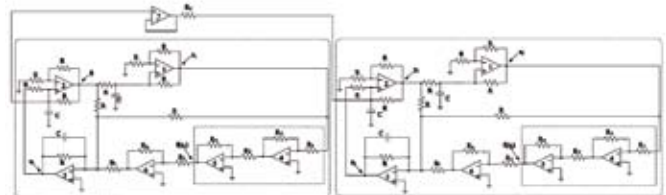


Figure 1. The schematic of the double-scroll circuits, unidirectionally coupled via a linear resistor R_C .

$$\begin{cases} \dot{x}_1 = y_1 \\ \dot{y}_1 = z_1 \\ \dot{z}_1 = -\alpha \cdot x_1 - \alpha \cdot y_1 - b \cdot z_1 + c \cdot f(x_1) \\ \dot{x}_2 = y_2 \\ \dot{y}_2 = z_2 + \xi \cdot (y_1 - y_2) \\ \dot{z}_2 = -\alpha \cdot x_2 - \alpha \cdot y_2 - b \cdot z_2 + c \cdot f(x_2) \end{cases} \quad (1)$$

In the above equation system a, b, c , are parameters and are defined as follows:

* E-mail address: Stavros@physics.auth.gr

$$\alpha = (RC)^{-1} \quad b = (RC)^{-1} \quad c = (R_x C)^{-1} \quad (2)$$

Signals $x_{1,2}$, $y_{1,2}$, and $z_{1,2}$, represent voltages. The first three equations of system (Eqs.1) describe the master circuit, while the other three describe the slave one. The saturation function $f(x_{1,2})$, used in Eqs.1 is defined by the following expression:

$$f(x) = \begin{cases} 1, & \text{if } x \geq k \\ \frac{1}{k}x, & \text{if } -k \leq x < k \\ -1, & \text{if } x < -k \end{cases} \quad (3)$$

and it is realized by the circuit part inside the dotted frame in Fig.1. Similar implementations were proposed in [30-33]. However the present implementation forms a characteristic with two saturation plateaus at ± 1 and an intermediate linear part with slope $1/k$. The value of k was set 0.5. The coupling coefficient is

$$\xi = \frac{R}{2R_c} \quad (4)$$

and appears only in the slave equation set, since a unidirectional coupling is considered.

The values of the circuit elements were: $R=20k\Omega$, $R_1=25k\Omega$, $R_2=14.3k\Omega$, $R_3=R_4=1k\Omega$, $R_5=R_6=1k\Omega$, $R_x=10k\Omega$ and $C=1nF$. The voltages of the positive and negative power supplies were set to $\pm 15V$. It should be mentioned that all the operational amplifiers used, were LF411. The operational amplifier 6 implemented the function $-f(x)$. Consequently, $\alpha=0.5$, $b=0.5$ and $c=1$. These values ensure that both the master and slave circuits operate in a chaotic mode and exhibit a double scroll attractor [34].

3. Measurements

Since R_c determines the value of coupling coefficient ξ (Eq.4), it served as the system's control parameter. Its value range extended from almost zero up to $60k\Omega$. In this region each circuit remained chaotic, exhibiting a double scroll attractor. However, the coupled circuits exhibit a transition from full synchronization to complete desynchronization, passing through a region of incomplete synchronization. The dynamics associated to this transition were proved to be that of on-off intermittency [35], [36]. Tab.1 presents in detail, the regions and the corresponding behavior in accordance to the control parameter. As deduced from this table, the critical value for which intermittent synchronization begins was found to be $R_{crit}=5.75k\Omega$.

Table 1. Synchronization Regions

Regions	Behavior	Control Parameter Value
Region I	Synchronization	$R_c < 5.75k\Omega$
Region II	Intermittent Synchronization	$5.75k\Omega \leq R_c \leq 60.00k\Omega$
Region III	Desynchronization	$R_c > 60.00k\Omega$

A four channel digital oscilloscope (Yokogawa DL9140) was used to register voltage signals x_1 , x_2 and y_1 , y_2 , in both sub-circuits, as well as, the difference signal $[x_1(t) - x_2(t)]$, that depicted the system synchronization. Synchronization phase portrait (x_1 vs. x_2) and each separate circuit phase portrait (x_1 vs. y_1 and x_2 vs. y_2) could also be acquisitioned, simultaneously.

In order to perform the related statistics, the difference signal $[x_1(t) - x_2(t)]$ was registered into a second digital oscilloscope (Tektronix TDS1002B) that was further connected to a laptop, facilitating the software needed for the evaluation. It should be mentioned that during measurements the oscilloscope was controlled by this laptop. For this reason a custom-made acquisition setup [37], based on NI's LabView, was created.

As long the circuit was operating in Region I, both the sub-circuits remained fully synchronized. In Fig.2a the time-series $x_1(t)$, $x_2(t)$ of both circuits, together with the difference signal $[x_1(t) - x_2(t)]$, are presented. In Fig.2b the individual phase portrait of each sub-circuit (x_1 vs. y_1 and x_2 vs. y_2) is shown. As expected in the case of complete synchronization, both the time-series and the corresponding circuit attractors are identical. The difference signal (Fig.2a) is continuously almost zero. As a result, in the synchronization portrait of $x_1(t)$ vs. $x_2(t)$ the trajectories remain strictly on the diagonal (Fig.2c).

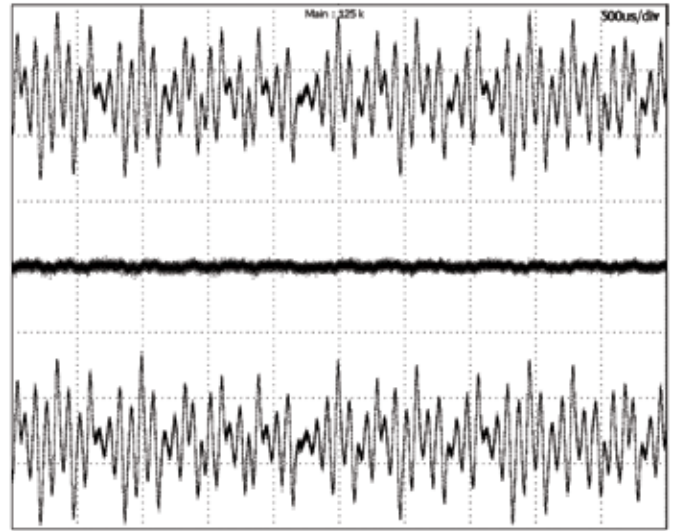


Figure 2a.

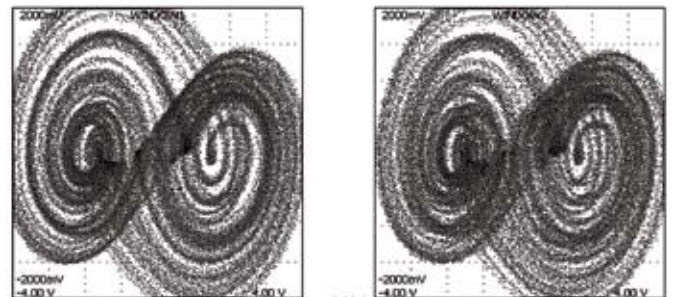


Figure 2b.

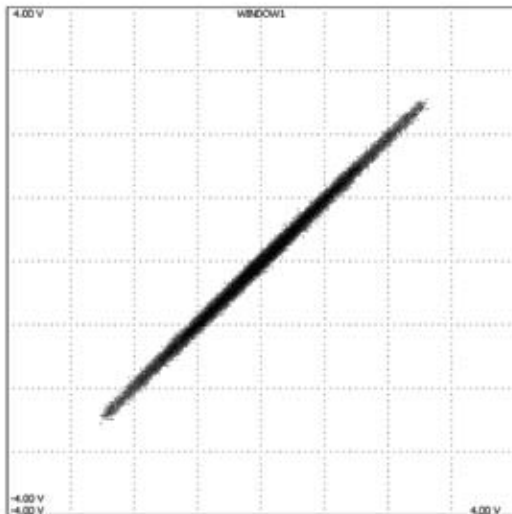


Figure 2c.

Figure 2. In the case of complete synchronization: (a) Time-series $x_1(t)$ (upper side), $x_2(t)$ (lower side) of both circuits, together with their difference signal $[x_1(t) - x_2(t)]$ (in the middle), (b) the phase portraits of each double scroll sub-circuit, (c) the synchronization portrait.

For values higher than R_{crit} , the system behavior enters Region II, in which the two sub-circuits are incompletely (intermittently) synchronized. The time-series $x_1(t)$, $x_2(t)$ of both circuits, together with their difference signal $[x_1(t) - x_2(t)]$ and the corresponding phase portraits (x_1 vs. y_1 and x_2 vs. y_2) are presented in Fig.3a and Fig.3b, respectively. The difference signal (Fig.3a) is almost zero for long time spaces, bursting occasionally at significantly non-zero values. These bursts become of longer duration and appear more frequently, with increasing values of the control parameter R_C . As expected in the case of incomplete synchronization, both the time-series and the attractors are intermittently correlated. This is confirmed in Fig.3b, where both sub-circuit, double scroll, attractors are quite similar; a careful examination reveals that they are not identical, though. Further corroboration is provided by the synchronization portrait of $x_1(t)$ vs. $x_2(t)$, where the trajectories remain for most of the time on the diagonal, escaping occasionally out of it (Fig.3c). It should be noted that although the two sub-circuits are intermittently synchronized they always operate in a chaotic mode.

Further corroboration is provided by the synchronization portrait of $x_1(t)$ vs. $x_2(t)$, where the trajectories remain for most of the time on the diagonal, escaping occasionally out of it (Fig.3c). It should be noted that although the two sub-circuits are intermittently synchronized they always operate in a chaotic mode.

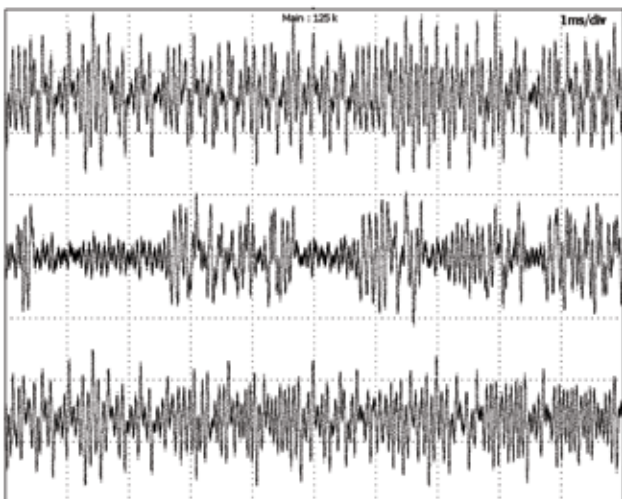


Figure 3a.

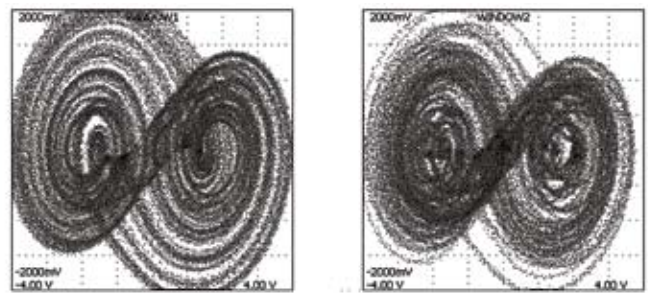


Figure 3b.

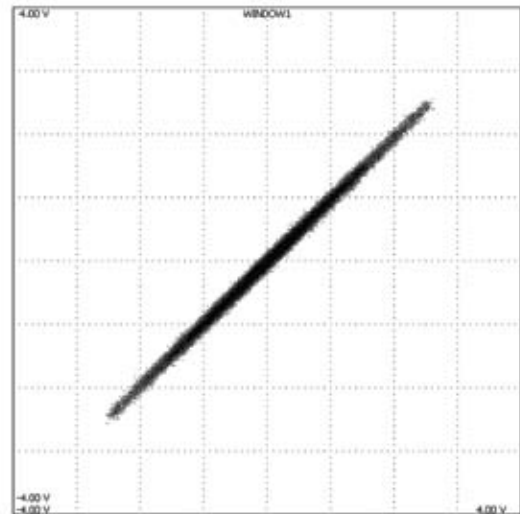


Figure 3c.

Figure 3. In the case of intermittent synchronization: (a) Time-series $x_1(t)$ (upper side), $x_2(t)$ (lower side) of both circuits, together with their difference signal $[x_1(t) - x_2(t)]$ (in the middle), (b) the phase portraits of each double scroll sub-circuit, (c) the synchronization portrait.

For $R_C > 60.00k\Omega$ the system operates in Region III. Although the two sub-circuits exhibit a chaotic behavior are fully desynchronized. In Fig.4a the time-series as well as their difference are shown, while in Fig.4b the chaotic attractors of each sub-circuit are presented. In this case of full desynchronization, the time-series and the attractors are continuously uncorrelated, as confirmed by the difference signal, which possesses almost always non-zero values. Consequently, the attractors of each double-scroll circuit

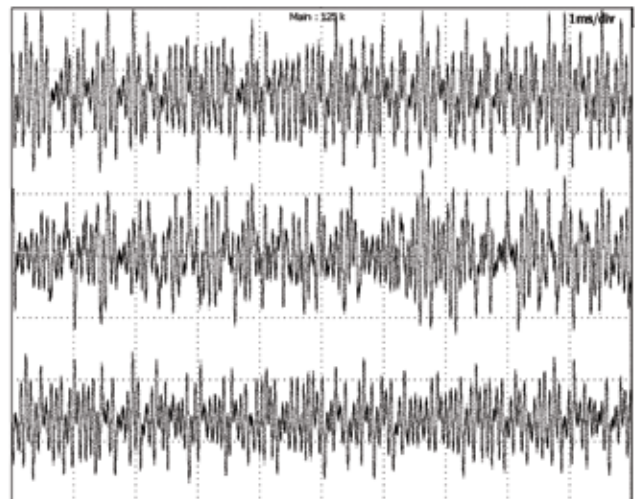


Figure 4a.

are completely different. Confirmation of this uncorrelated behavior, where the trajectories remain for almost all of the time out of the diagonal, is provided by the (de-)synchronization portrait of $x_1(t)$ vs. $x_2(t)$ (Fig.4c).

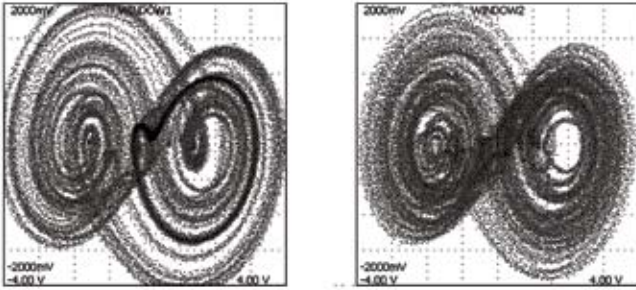


Figure 4b.

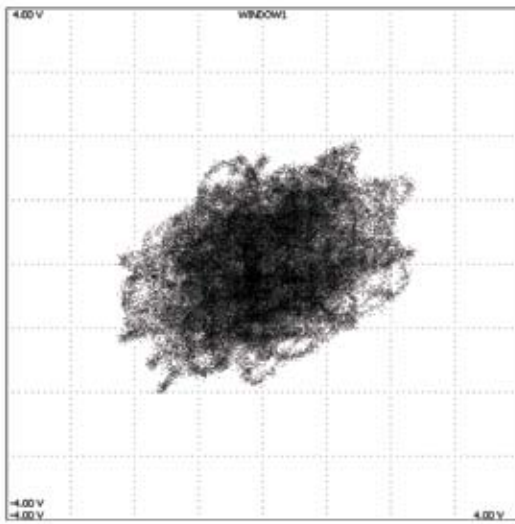


Figure 4c.

Figure 4. In the case of complete desynchronization: (a) Time-series $x_1(t)$ (upper side), $x_2(t)$ (lower side) of both circuits, together with their difference signal [$x_1(t) - x_2(t)$] (in the middle), (b) the phase portraits of each double scroll sub-circuit, (c) the (de-)synchronization portrait.

4. Evaluation

To gain an insight of the mechanism governing the transition from full synchronization to complete desynchronization in the studied master-slave system, the laminar length distributions and the scaling of the mean laminar lengths with the difference $(R_C - R_{Ccrit})$, were examined.

In a first step, the distribution $P(\tau)$ of durations τ of laminar lengths of the difference signal, is presented in a double logarithmic plot, for the representative case with coupling resistance $R_C=30.00k\Omega$ (Fig.5). The curve of this plot consists mainly of a linear part with slope β equal to -1.496, though in the range of large laminar lengths, the distribution exhibits an exponential decay. Apparently, in the linear part of this distribution, probability $P(\tau)$ scales with τ with the exponential factor β [38-40]:

$$P(t) \propto t^\beta \quad (5)$$

holding for exponent value $\beta = -1.50$. In the mentioned case of $R_C=30.00k\Omega$, β deviates from the predicted value, only by 0.3%. Similar distributions for other values of control parameter R_C gave slopes β (for the linear part) not substantially deviating from -1.50, as well as an exponential decay in the range of large τ [42]. These values support the classification of the observed incomplete synchronization in the “On-Off Intermittency” class.

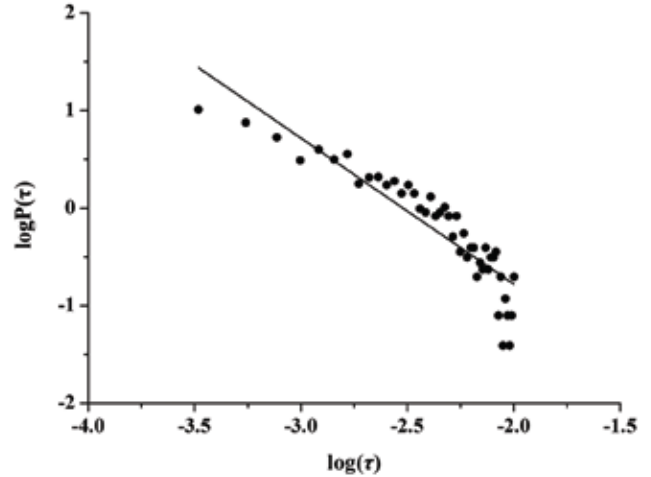


Figure 5. A representative ($R_C=30k\Omega$) distribution $P(\tau)$ of durations τ of laminar lengths in a double logarithmic plot. Full circles denote experimental data, while the line represents a fitting with a power law of the form of Eq. (5).

In a second instance, mean duration $\langle \tau \rangle$ of laminar lengths vs. the difference $(R_C - R_{Ccrit})$ was checked. The corresponding results are presented in a double logarithmic plot, in Fig.6. A least square fitting of the experimental data leads to a straight line with a slope γ equal to -1.093, clearly confirming the following power law [37], [39]:

$$\langle t \rangle \propto (R_C - R_{Ccrit})^\gamma \quad (6)$$

This law predicts a scaling of $\langle \tau \rangle$ with the difference $(R_C - R_{Ccrit})$ with $\gamma = -1.0$. The obtained value for γ deviates by 9.3% from

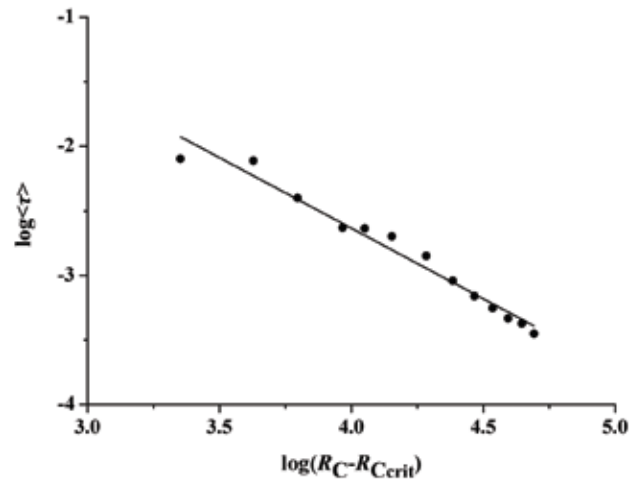


Figure 6. Double logarithmic plot of the mean duration $\langle \tau \rangle$ of laminar lengths vs. the difference $(R_C - R_{Ccrit})$. Full circles denote experimental data, while the line represents fitting with a power law of the form of Eq. (6).

the theoretically foreseen one. This result is in full accordance with the classification of the observed intermittency as an “On–Off” type [41-43].

5. Conclusions

In this report the route from synchronization to desynchronization of two identical double-scroll circuits, unidirectionally coupled, was experimentally studied. The present realization of the double-scroll circuits differs from the usually used elsewhere, in such a way that the saturated plateaus at $\pm 1V$ are connected by a straight line with slope of $1/k$. This implementation offers the advantage of a rather smooth transition between the two plateaus avoiding premature and overdue jumps between them, as it is often the case in the precipitous transition between them.

The related evaluation of the experimental results led to the conclusion that desynchronization of this master-slave circuit

demonstrated the typical behavior theoretically predicted for the case of “On–Off” intermittency [41], [42]. In specific, the distributions $P(\tau)$ of durations τ of laminar lengths of the difference signal, were found to scale with an exponent $\beta \approx 1.5$; while the mean duration $\langle \tau \rangle$ of laminar lengths was found to scale with an exponent $\gamma \approx 1$.

In this case of unidirectional coupling, the desynchronization phenomenon scaled into a narrower range (up to $60k\Omega$) compared to the bidirectional case (up to $90k\Omega$) [34]. This expected, since in unidirectional coupling the master circuit dynamics evolve independently while the slave circuit dynamics evolution is influenced by the master. This results to earlier desynchronization. On the contrary, in bidirectional coupling both the circuits influence one another, resulting to putting back full desynchronization. What is noteworthy is that in both cases of bidirectional and unidirectional, resistive coupling, desynchronization was coming up by following the “On–Off” intermittency dynamics.

References

1. G. Chen, X. Dong, From chaos to order: methodologies, perspectives and applications, World Scientific, Singapore (1998).
2. G. Chen, X. Yu, Chaos control: theory and applications, Springer-Verlag, Berlin, Heidelberg (2003).
3. L. M. Pecora and T. L. Carroll, Phys. Rev. Lett. 64, 821 (1990).
4. J. M. González-Miranda, Synchronization and control of chaos: An introduction for scientists and engineers, Imperial College Press, London (2004).
5. C. Cruz-Hernandez and N. Romero-Haros, Commun. Nonlinear Sci. Numer. Simul. 13, 645 (2008).
6. L. Kocarev and U. Parlitz, Phys. Rev. Lett. 74, 5028 (1995).
7. G. Kolumban, M. P. Kennedy and L. O. Chua, IEEE Trans. Circ. Syst. I 44, 927 (1997).
8. A. S. Dmitriev, A. V. Kletsov, A. M. Laktushkin, A. I. Panas and S. O. Starkov, Uspekhi Sovremennoi Radioelektroniki 1, 4 (2008).
9. M. Hasler, Int. J. Bifurcat. Chaos 8, 647 (1998).
10. G. Alvarez, F. Montoya, M. Romera and G. Pastor, Proc. 33rd Annual 1999 Int. Carnahan Conference on Security Technology, 332 (1999).
11. C. P. Silva and A. M. Young, Proc. IEEE Aerospace Conference, 279 (2000).
12. L. Kocarev, IEEE Circ.Syst.Mag 1, 6 (2001).
13. C.K. Tse and F.C.M. Lau, Chaos-based digital communication systems: operating principles. Analysis methods and performance evaluation, Springer-Verlag, Berlin, Heidelberg (2003).
14. Ch. K. Volos, I. M. Kyprianidis and I. N. Stouboulos, WSEAS Trans. Circ. Syst. 5, 1654 (2006).
15. L. O. Chua, C. W. Wu, A. Huang and G. Q. Zhong, IEEE Trans. Circ. Sys. I 40, 7321 (1993).
16. I. M. Kyprianidis, Ch. K. Volos and I.N. Stouboulos, Proc. I Interdisciplinary Chaos Symposium, 4, 45 (2006).
17. K. S. Tsang and K. F. Man, Proc. IEEE Int. Symposium on Industrial Electronics, 441 (1998).
18. K. S. Tsang and K. F. Man, IEEE Trans.Circ.Syst. I 48, 635 (2001).
19. A. S. Elwakil and M. P. Kennedy, IEEE Trans.Circ.Syst. I 47, 76 (2000).
20. A.S. Elwakil, K.N. Salama and M.P. Kennedy, Proc. IEEE Int. Symposium on Circuits and Systems, V, 217 (2000).
21. Ch. K. Volos, I. M. Kyprianidis and I. N. Stouboulos, J. Appl. Funct. Anal. 4, 703 (2008).
22. I. M. Kyprianidis and I. N. Stouboulos, Chaos Solitons Fract. 17, 317 (2003).
23. I. M. Kyprianidis, Ch. K. Volos, I. N. Stouboulos and J. Hadjidemetriou, Int. J. Bifurcat. Chaos 16, 1765 (2006).
24. I. M. Kyprianidis, Ch. K. Volos and I. N. Stouboulos, Nonlinear Phenom. Complex Syst. 11, 187 (2008).
25. A. N. Miliou, I. P. Antoniadis, S. G. Stavriniades and A. N. Anagnostopoulos, Nonlinear Anal: Real World Appl. 8, 1003 (2007).
26. I. P. Antoniadis, A. N. Miliou, S. G. Stavriniades and A. N. Anagnostopoulos, J. Appl. Funct. Anal. 4, 237 (2009).
27. A. N. Miliou, S. G. Stavriniades, A. P. Valaristos and A. N. Anagnostopoulos, Nonlinear Anal: Theory Methods Appl. 71, e21 (2009).
28. S. G. Stavriniades, A. N. Miliou, A. N. Anagnostopoulos, V. Konstantakos, Th. Laopoulos and L. Magafas, Chaos Solitons Fract. 42, 33 (2009).
29. S. G. Stavriniades, A. N. Anagnostopoulos, A. N. Miliou, A. Valaristos, L. Magafas, K. Kosmatopoulos and S. Papaioannou, J. Eng. Sci. Rev. 2, 82 (2009).
30. A. C. J. Luo, Commun. Nonlinear Sci. Num. Simul. 14, 1901 (2009).
31. A. S. Elwakil, K. N. Salama and M. P. Kennedy, Proc. IEEE Int. Symposium on Circuits and Systems (ISCAS'00) 5, 217 (2000).
32. A. S. Elwakil, K. N. Salama and M. P. Kennedy, Int. J. Bifurcat. Chaos 6, 2885 (2002).
33. J. Lü, G. Chen, X. Yu and H. Leung, IEEE Trans. Circ. Syst. I 51, 2476 (2001).
34. I. M. Kyprianidis, Ch. K. Volos, S. G. Stavriniades, I. N. Stouboulos and A. N. Anagnostopoulos, Commun. Nonlinear Sci. Num. Simul. doi:10.1016/j.cnsns.2009.09.007 (2009).
35. N. Platt, E. A. Spiegel and C. Tresser, Phys. Rev. Lett. 70, 729 (1993).
36. P.W. Hammer, N. Platt, S.M. Hammel, J.F. Heagy and B.D. Lee, Phys. Rev. Lett. 73, 1095 (1994).
37. S. G. Stavriniades, V. Konstantakos, Th. Laopoulos, A. N. Anagnostopoulos and A. Valaristos, Proc. IEEE IDAACS'09 (Italy), 111 (2009).
38. E. Ott, Chaos in Dynamical Systems-2nd Edition, Cambridge University Press, Cambridge (2002).
39. A. Cenys, A. Namajunas, A. Tamacevicius and T. Schneider, Phys. Lett. A 213, 259 (1996).
40. A. Pikowsky, M. Rosenblum and J. Kurths, Cambridge University Press, Cambridge (2003).
41. C. Toniolo, A. Provenzale and E. A. Spiegel, Phys. Rev. E 66, 066209 (2002).
42. Q. Chen, Y. Hong, G. Chen and D. J. Hill, IEEE Trans. Circ. Syst. I 53, 2692 (2006).
43. J. F. Heagy, N. Platt and S. M. Hammel, Phys. Rev. E 49, 1140 (1994).